

## Theoretical and experimental studies on the coordination ability of 1,4-bis(dimethylphosphinylmethylenoxy)benzene

P. J. Gorolomova<sup>1</sup>, R. P. Nikolova<sup>2</sup>, B. L. Shivachev<sup>2</sup>, V. I. Ilieva<sup>1</sup>, D. Ts. Tsekova<sup>1</sup>, T. D. Tosheva<sup>3</sup>, E. S. Tashev<sup>3</sup>, S. G. Varbanov<sup>4</sup>, G. G. Gencheva<sup>1,\*</sup>

<sup>1</sup> Faculty of Chemistry, University of Sofia, 1164 Sofia, Bulgaria

<sup>2</sup> Institute of Mineralogy and Crystallography, Bulgarian Academy of Sciences, 1113 Sofia, Bulgaria

<sup>3</sup> Institute of Polymers, Bulgarian Academy of Sciences, 1113 Sofia, Bulgaria

<sup>4</sup> Institute of Organic Chemistry with Center of Phytochemistry, Bulgarian Academy of Sciences, 1113 Sofia, Bulgaria

Received January 28, 2011; Revised April 22, 2011

Combined experimental and theoretical study of the crystal, molecular and electronic structure, and coordination ability of 1,4-bis(dimethylphosphinylmethylenoxy)benzene was performed using X-ray single-crystal analysis, FT-IR spectral characterization and quantum chemical calculations. The title compound crystallizes in the triclinic crystal system, P-1 space group. The asymmetric unit consists of two symmetrically independent molecules. The optimization of the molecular structure of the compound in gas phase at different levels of theory (ab initio, RHF/6-311G(d), MP2/6-311G(d) and DFT B3LYP/6-311G(2df,2p)) shows existence of several conformers. In the description of the conformers, a torsion angle  $C_{Ar}-C_{Ar}-O-C$  was used. The results from the optimized molecular structures are compared with the X-ray single crystal data. The electronic structure of the most important for the coordination ability molecular fragments, was described in terms of Natural Bond Orbitals (NBO) analysis and Mulliken charges.

**Key words:** X-ray diffraction, conformation analysis, chemical reactivity, tertiary phosphine oxides.

### INTRODUCTION

Dimethyl(methylenoxyaryl)phosphine oxides [1] are a relatively small group of organophosphorous compounds that belongs to the family of the tertiary phosphine oxides. The tertiary phosphine oxides are used widely in generation of Wittig-Horner reagents [2], as building blocks in organic synthesis [3] and intermediates for the design of nano-electronic and supramolecular materials [4]. In recent years, there has been considerable interest in the studying their coordination behavior to transition and lanthanide ions [5], because those of them having bulky and branched substituents are very suitable for extraction of rare-earth and transuranic elements [6]. Therefore, the current research on the coordination ability and reactivity of a series of bis(dimethylphosphinylmethylenoxy)benzenes [7], whose representative is the title compound (Fig. 1) is timely and important, in order to evaluate their potential application in separation chemistry as well as for synthesis of

new materials. The presented paper describes the experimental and theoretical studies of the crystal, molecular and electronic structure of one of these isomers, namely 1,4-bis(dimethylphosphinylmethylenoxy)benzene (*p*-I) and discusses its coordination ability.

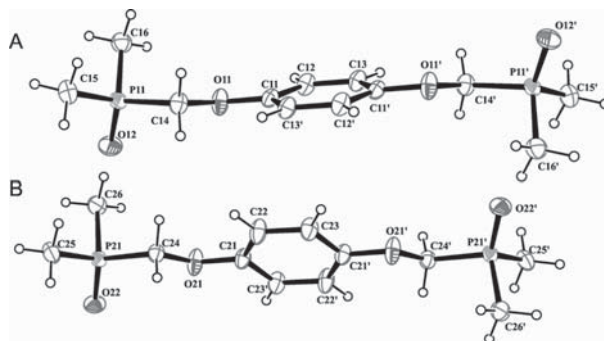


**Fig. 1.** An ORTEP view (ellipsoids at 50% probability) of 1,4-bis(dimethylphosphinyl-methylenoxy)benzene with atom labeling scheme. H atoms are shown as small spheres of arbitrary radii

\* To whom all correspondence should be sent:  
E-mail: ahgg@chem.uni-sofia.bg

## EXPERIMENTAL

*Crystal growth*

Colorless prismatic crystals of 1,4-bis(dimethylphosphinylmethyleneoxy)benzene suitable for X-ray diffraction were obtained during the interaction of  $\text{CuCl}_2$  with a fourfold excess of the title compound in  $\text{C}_2\text{H}_5\text{OH}$  (96%). The experimental IR spectrum of p-I was recorded on a ALPHA FT-IR spectrometer – Bruker Optics. IR ( $\text{cm}^{-1}$ ): 1501, 1437, 1416  $\nu(\text{Ar}(\text{C}=\text{C}))$ ; 1291; 1221  $\nu(\text{C}_{\text{Ar}}-\text{O})$ ; 1163  $\nu(\text{P}=\text{O})$ ; 1043  $\nu(\text{CH}_2-\text{O})$ ; 932, 896, 866, 835  $\delta(\text{CH}_3-\text{P}-\text{CH}_3) + \delta(\text{CH}_2-\text{P}-\text{CH}_3)$ ; 822; 742; 523; 404.

*Single crystal X-ray analysis*

A prismatic crystal of the title compound having approximate dimension of  $0.28 \times 0.24 \times 0.24$  mm was placed on a glass fiber and mounted on an Enraf-Nonius CAD-4 diffractometer. X-ray data collection was carried out at room temperature with graphite monochromatized Mo-K $\alpha$  radiation ( $\lambda = 0.71073$  Å). The unit cell parameters were determined from 15 reflections and refined employing 22 higher-angle reflections,  $17 < \theta < 20^\circ$ . The  $\omega/2\theta$  technique was used for data collection using Nonius Diffractometer Control Software [8]. Lorentz and polarization corrections were applied to intensity data using the WinGX [8]. The structure was solved by direct methods using SHELXS-97 [8] and refined by full-matrix least-squares procedure on  $F^2$  with SHELXL-97 [8]. The hydrogen atoms were placed in idealized positions ( $C_{\text{aromatic}} = 0.93$ ,  $C_{\text{methyl}} = 0.97$  and  $C_{\text{methylene}} = 0.96$  Å) and were constrained to

**Table 1.** Crystal data and structure refinement indicators for 1,4-bis(dimethylphosphinylmethyleneoxy)benzene

Empirical formula	$\text{C}_{12}\text{H}_{20}\text{O}_4\text{P}_2$
Molecular weight	290.22
Crystal size (mm)	$0.28 \times 0.24 \times 0.24$
Crystal system	Triclinic
Space group	$P-1$
T(K)	290
Radiation wavelength (Å)	0.71073 (Mo K $\alpha$ )
$a$ (Å)	6.202(3)
$b$ (Å)	9.290(6)
$c$ (Å)	13.356(9)
$V$ (Å $^3$ )	728.1(8)
$Z$	2
$\alpha$ ( $^\circ$ )	100.066(12)
$\beta$ ( $^\circ$ )	100.788(12)
$\gamma$ ( $^\circ$ )	99.675(11)
$d$ ( $\text{mg. m}^{-3}$ )	1.324
$\mu$ ( $\text{mm}^{-1}$ )	0.302
Reflections collected/unique	5628/2873
$R1$ ( $I > 2\sigma(I)$ )	0.056
$wR2$ (all data)	0.164

ride on their parent atoms, with  $U_{\text{iso}}(\text{H}) = 1.2U_{\text{eq}}(\text{C})$ . The X-ray diffraction data and details concerning data collection and structure refinement are given in Table 1, ORTEP diagram of p-I is shown on Fig. 1

*Computational Details*

The molecular and electronic structures of 1,4-bis(dimethylphosphinyl-methyleneoxy)benzene were obtained by DFT (Becke's 3-Parameter hybrid functional combined with the Lee-Yang-Parr correlation functional B3LYP [9]) and *Ab initio* (Restricted Hartree-Fock Method (RHF) [10] and second-order Møller-Plesset perturbation theory (MP2) [11]) calculations (full optimization in gas phase) using Gaussian 09 software package [12]. Several basis sets such as triple- $\zeta$  Pople type 6-311G(d), 6-311G(2df,2p) and double- $\zeta$  6-31G(d) [13] were employed for the calculations. The Natural Bond Orbitals (NBO) [14] calculations were performed with the NBO-code included in Gaussian09 [12]. The calculated vibrational frequencies of the compound (program package Gaussian09 [12]) were used to check the structural optimizations and to compare with experimental data.

## RESULTS AND DISCUSSION

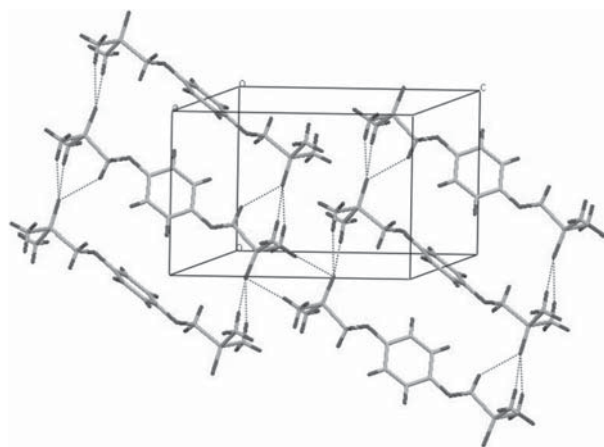
The title compound crystallizes in the centrosymmetric space group  $P-1$ . There are two symmetrically non equivalent p-I molecules (A and B) in the asymmetric unit Fig. 1. The observed bond lengths and angles in A and B are typical for such compounds [3a, 15], Table 2. The phosphorus atoms possess distorted tetrahedral arrangement with bond angles range between  $104.07(3) - 114.82(5)^\circ$  and relatively localized P=O double bonds (1,489 Å for (A) and 1,484 Å for (B)). The two *p*-disposed ether oxygen atoms O11 and O11' as well as O21 and O21' also share the least-squares aromatic plane with an equal deviation of **0.003** Å. The A and B moieties are arranged in such a matter to minimize the steric hindrance of the bulky methyl groups Fig. 2. The angle between the mean planes of the aromatic rings of A and B is  $55.11(4)^\circ$ . In addition, very weak C-H(methyl)...O intermolecular interactions are observed. As a consequence of the crystal packing, the dihedral angles C-O-C $_{\text{Ar}}$ -C $_{\text{Ar}}$  in the A and B type molecules differ about  $6.5^\circ$  and these of O12-P11-C14-O11 – about  $14.5^\circ$ .

*Geometry optimization of the molecular structure and conformation analysis*

Despite of the accuracy of the X-ray data in the determination of the molecular geometry of the

**Table 2.** Selected geometrical parameters (distances in Å and angles in degrees) of p-I

Parameter	Crystal structure		Optimized structure / Methods		
	A	B	RHF	B3LYP	MP2
<i>Dihedral angles (°)</i>					
O12-P11-C14-O11	-50.22(0)	-64.76(0)	+180.00	+180.00	+177.89
P11-C14-O11-C11	-178.77(0)	+178.37(0)	+179.99	+180.00	-91.88
C14-O11-C11-C12	-157.91(0)	+164.77(0)	+0.02	0.00	-5.61
C14'-O11'-C11'-C13	+157.91(0)	-164.77(0)	-179.98	+180.00	175.22
<i>Bond angles (°)</i>					
C12-C11-O11	125.15(0)	125.04(0)	115.84	115.74	114.76
C13'-C11-O11	115.64(0)	115.52(0)	124.97	124.75	126.20
C11-O11-C14	117.13(0)	117.21(0)	119.82	118.36	118.63
O11-C14-P11	108.11(0)	108.53(0)	109.33	110.18	115.20
C14-P11-O12	113.77(0)	114.82(0)	110.82	110.49	111.75
C14-P11-C15	114.38(0)	114.39(0)	104.99	103.87	102.20
C14-P11-C16	105.13(0)	104.07(0)	104.99	104.83	106.48
C15-P11-O12	114.38(0)	114.39(0)	114.72	115.52	115.93
C15-P11-C16	107.22(0)	106.54(0)	105.71	102.72	103.94
C16-P11-O12	112.83(0)	113.58(0)	114.71	115.51	115.26
<i>Bond Length ?</i>					
C11-O11	1.377(0)	1.375(0)	1.358	1.376	1.376
O11-C14	1.412(0)	1.423(0)	1.398	1.420	1.420
C14-P11	1.832(0)	1.846(0)	1.832	1.846	1.845
P11-O12	1.489(0)	1.484(0)	1.469	1.489	1.498
P11-C15	1.785(0)	1.777(0)	1.810	1.818	1.811
P11-C16	1.785(0)	1.786(0)	1.800	1.818	1.811

**Fig. 2.** Packing of the molecules within the unit cell down the b-axis. Intermolecular interactions are marked with dashed lines.

studied compound, to estimate fully its electronic structure and coordination behavior, theoretical analysis was applied. Generally, the molecule possesses two types of coordination centers: the phosphoryl oxygen atoms as well as the ether oxygen atoms. In addition, the bond lengths of the P=O units are indicative for localized double bonds [15] and hence it could be expected relatively limited coordination ability of the phosphoryl oxygen atoms.

The computational modelling of the molecular and electronic structure of 1,4-bis(dimethylphosphorylmethyleneoxy)-benzene was performed in gas phase using different levels of theory: RHF/6-311G(d) and MP2/6-311G(d) and DFT B3LYP/6-311G(2df,2p) (Fig. 3). All theoretical found bond lengths and bond angles are in agreement with X-ray refinements values (Table 2). However, significant differences were observed for the torsion angles. The optimized structures obtained using RHF/6-311G(d) and B3LYP/6-311G(2df,2p) are close but differ significantly of that obtained by MP2/311G(d) (Table 2, Fig. 3). Moreover, each of them differs from the experimental single-crystal data. The differences relate to the positions of the two substituents in respect to the plane of the benzene ring. In addition, if we compare the experimentally determined dihedral angles and these obtained after geometry optimization using the Z-matrix from the X-ray diffraction, torsion relaxations were also observed (Fig. 4.). Thus in gas phase, free from the intermolecular forces, the molecules relax to the nearest local minima in the potential surface. It is evident that the observed large degree of structural mobility is due to the three single bonds C(Ar)-O-C-P in each substituent. In order to characterize the stable conformational states, the potential energy profile for the internal rotation around C<sub>Ar</sub>-O was calculated. In the description of the conformers, the

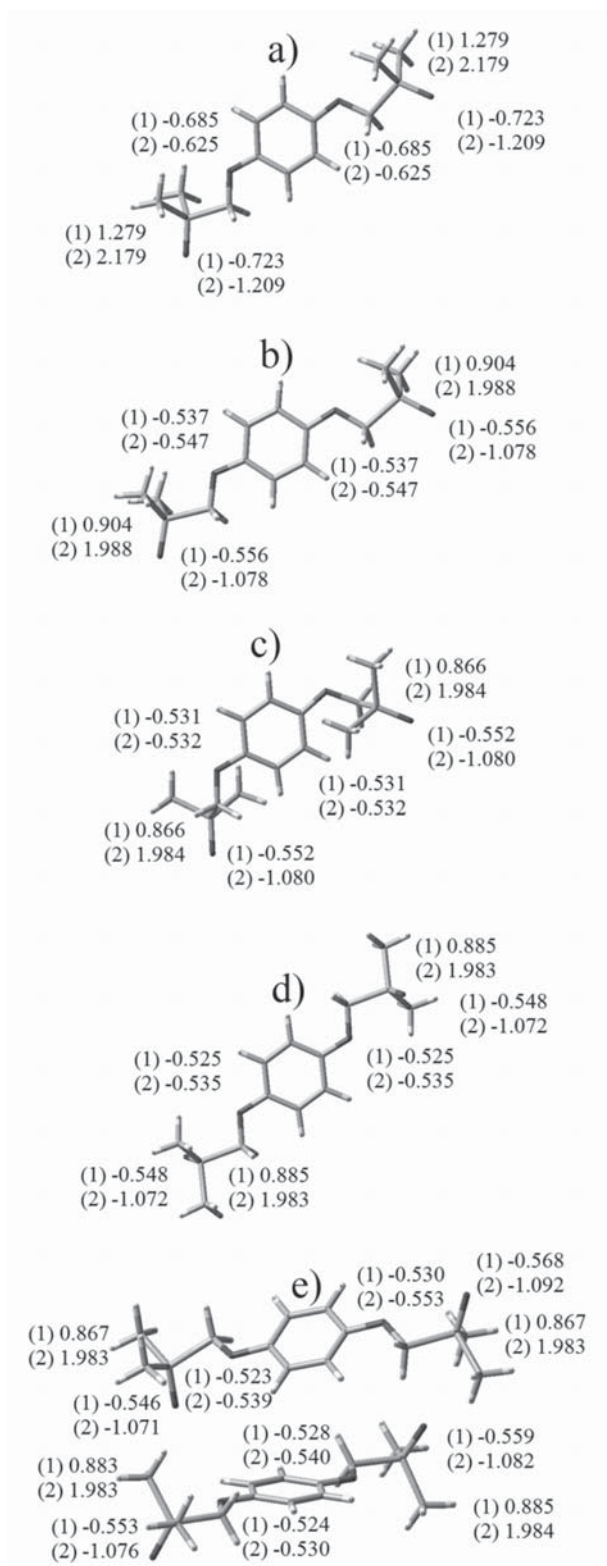


**Fig. 3.** Optimized structure of 1,4-bis(dimethylphosphinylethyleneoxy)benzene with depicted values of the Mulliken (1) and NPA (2) charges, obtained using: a) RHF/6-311G(d); b) B3LYP/6-311G(2df,2d); c) MP2/6-311G(d); d) Z-matrix of X-ray data for an isolated A molecule at B3LYP/6-31G(d); e) Z-matrix of X-ray data of the two molecules in the unit cell at B3LYP/6-31G(d)



**Fig. 4.** Molecular structure of isolated A molecule using X-ray data: a) single point structure, b) after optimization (the optimization was carried out without any restrictions on the symmetry)

torsion angle between the benzene ring and the O11-C14 bond, namely  $C_{Ar}-C_{Ar}-O-C$  ( $\phi$ , C12-C11-O11-C14) was used (Fig. 5). The opposite dihedral angle (C12'-C11'-O11'-C14') in the second substituent has values around  $-179.5^\circ$  or  $+179.5^\circ$ .

B3LYP/6-31G(d) calculations predict the existence of more than five conformations (Fig. 5). The estimated conformational energy differences are very small ( $<3$  kJ/mol) and only between the most stable conformer ( $\phi \sim 150^\circ$ ) and the least stable one ( $\phi \sim 30^\circ$ ), the energy difference is  $\sim 11.5$  kJ/mol (Fig. 5). Hence, on the basis of the theoretical results, the existence of several relative stable conformers could be expected.

The minima obtained by the theoretical scan were optimized. The five relevant lowest energy conformers found are depicted on Fig. 6. Their calculated parameters together with these obtained for the optimized molecule structures on the basis of the Z-matrix of the X-ray data for an isolated A molecule as well as for A and B molecules in the unit cell are presented in Tables 3. The calculated data for the minimized energies listed in Table 3 show that the highest symmetric conformer d) with dihedral angles  $\phi_1 = C_{14}-O_{11}-C_{11}-C_{12}$  and  $\phi_2 = C_{14}'-$

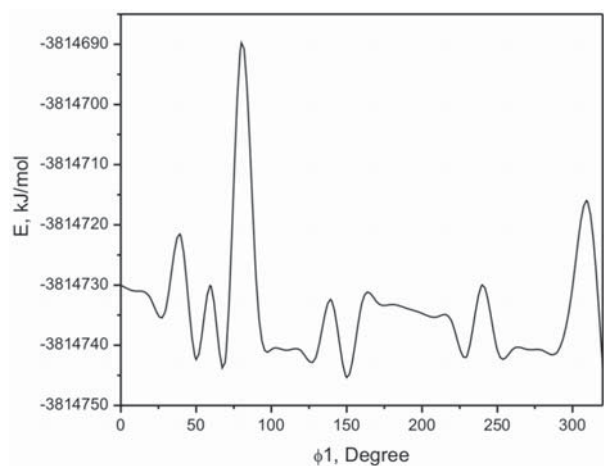


**Fig. 5.** Calculated potential energy curve for the rotation around the C11-O11 single bond

$O_{11}$ ,  $C_{11}$ ,  $C_{13}$  +180° and -180° is the most stable one among the various conformers. This conformer is with 1.6 kJ/mol more stable, than the optimized molecules, obtained after geometric optimization of the Z-matrix of X-ray data (the calculated total

energy is presented per one molecule) and 20.8 kJ/mol more stable than the optimized molecular structure of the isolated A-molecule.

In order to appraise the coordination ability of the compound, its molecular structure was interpreted from the electronic point of view. Selected results from the natural population analysis of the five conformers together with the molecule structures obtained from optimization of the X-ray determined Z-matrix are presented in Tables 3 and 4.

The discussion is focused on the lone pair orbitals (LP) of ether oxygen and phosphoryl oxygen atoms as well as on their principal localization quantitatively estimated through second order perturbation energy stabilization (see Table 3). The one-centre valence lone pairs (LP) orbitals are appropriate for co-ordination to metal ions. One LP orbital on ether oxygens and two LP orbitals of phosphoryl oxygens have mainly p-character and they are practically occupied by two electrons. Natural bond orbital (NBO) analysis provides a description of the molecular structure by a set of localized two-center bond and antibond orbitals as well as one-center core pair, valence lone pair and Rydberg extravalence orbitals. The analysis of the stabilizing interactions between filled and unoccupied as well as destabilizing interactions between filled orbitals based on the data of the Fock matrix in the NBO basis is useful to estimate the hyperconjugation and delocalization in the molecule structure. In this study, DFT level computation was used to investigate the second-order interaction between the oxygen LP orbitals and proper vacant antibonding orbitals as a measure for the lone pair localization (Table 4) and potential coordination ability. The natural orbital interactions were analyzed with the NBO Version 3.1 [14]. Since these interactions lead to donation of occupancy from the localized NBOs of the idealized Lewis structure into the empty non-Lewis orbitals, they refer to the “delocalization” corrections to the zeroth-order natural Lewis structure. For each donor NBO (*i*) and acceptor NBO (*j*), the stabilization energy *E2* as defined in [14e] is associated with the degree of *i* → *j* intramolecular hyperconjugative interactions and can be used as a measure of the engagement of the lone pairs in the intramolecular delocalization. The larger the *E2* values shows the more intensive interaction between electron donors and electron acceptors orbitals. The data about the interactions of  $n(O_{11}) \rightarrow \pi(C_{11}-C_{12})^*$  and  $n(O_{11}) \rightarrow \pi(C_{11}-C_{13})^*$  are related to resonance in the molecules due to electron donation from LP(O) of the ether oxygen atoms to anti-bonding acceptor  $\pi(C-C)$  of the phenyl ring. The large stabilization energy for these interactions (more than 103.8 kJ/mol, Table 4) shows high hyperconjugation between the electron donating ether oxygen and the phenyl ring. These

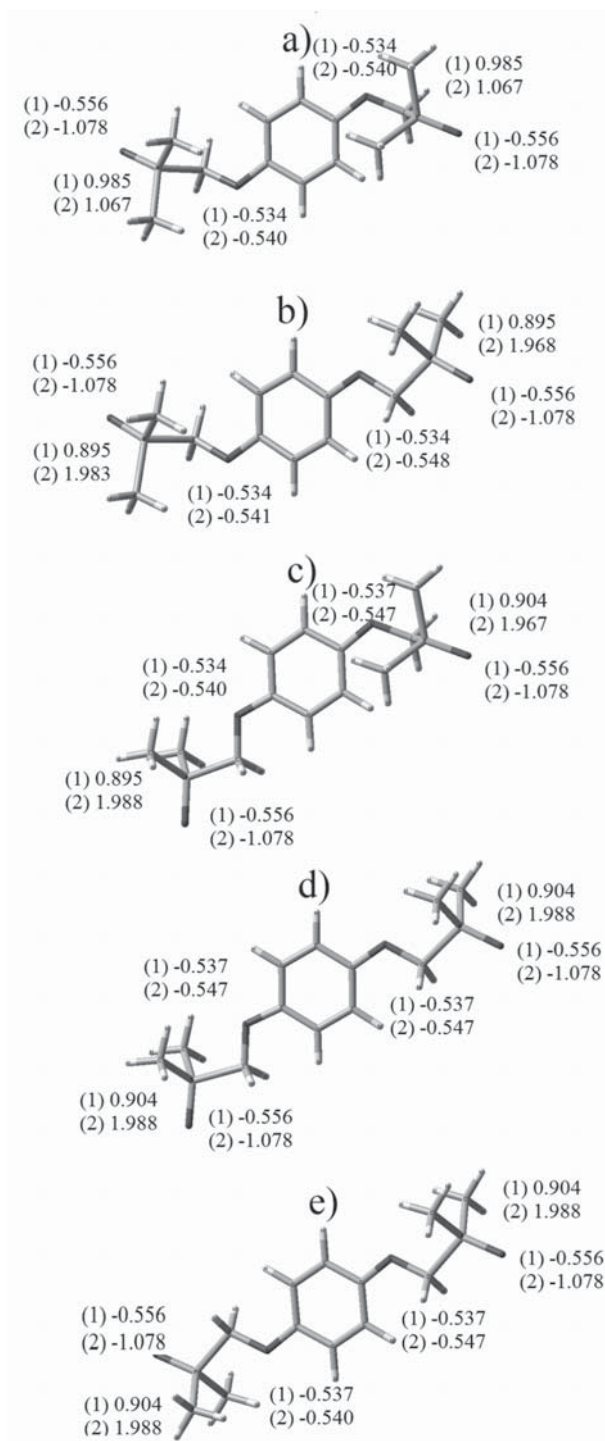


**Fig. 6.** The lowest energy conformers with depicted values of the Mulliken (1) and NPA (2) charges

**Table 3.** Theoretical parameters of the selected stable conformers and the optimized molecules using Z-matrix of X-ray data for the isolated A molecule, and A and B molecules in the crystallographic cell obtained by B3LYP/6-31G(d) level of theory (Dihedral angles  $\phi_1 = \text{C14-O11-C11-C12}$  and  $\phi_2 = \text{C14'-O11'-C11'-C13}$ ; \*-HOMO)

Conformation number	Parameter Molecular Energy [kJ/mol]	Dihedral Angles		Lone pair					
		$\phi_1$	$\phi_2$	LP(O11) Occupancy % p character Orbital Energy, [kJ/mol]	LP(O11') Occupancy % p character Orbital Energy, [kJ/mol]	LP1(O12) Occupancy % p character Orbital Energy, [kJ/mol]	LP2(O12) Occupancy % p character Orbital Energy, [kJ/mol]	LP1(O12') Occupancy % p character Orbital Energy, [kJ/mol]	LP2(O12'') Occupancy % p character Orbital Energy, [kJ/mol]
a)	-3814739.1	12.33	-170.61	1.85514 99.69 % p -849.9	1.85419 99.78 % p -848.6	1.80991 99.74 % p -619.8	1.79848 99.74 % p -620.0	1.81002 99.74 % p -620.1	*1.79836 99.74 % p -620.0
b)	-3814739.4	11.23	178.69	1.85463 99.73 % p -846.9	1.85974 99.92 % p -845.2	1.80985 99.74 % p -618.1	1.79813 99.74 % p -618.3	1.81097 99.74 % p -618.7	*1.79827 99.73 % p -619.1
c)	-3814740.0	179.74	-172.31	1.85903 99.92 % p -845.6	1.85298 99.84 % p -845.9	1.81094 99.74 % p -618.7	1.79826 99.73 % p -619.1	1.81020 99.74 % p -617.4	*1.79832 99.74 % p -617.5
d)	-3814750.9	180.00	-180.00	1.85904 99.92 % p -843.5	1.85904 99.92 % p -843.6	1.81092 99.74 % p -617.3	1.79819 99.73 % p -617.7	1.81092 99.74 % p -617.3	*1.79818 99.73 % p -617.7
e)	-3814750.2	0.03	179.98	1.85974 99.92 % p -842.9	1.85974 99.92 % p -842.9	1.91108 99.74 % p -617.3	1.79845 99.75 % p -617.8	1.81107 99.74 % p -617.4	*1.79844 99.74 % p -617.8
X-ray 1 mol	-3814730.1	177.38	3.02	1.85689 99.91 % p -821.9	*1.85689 99.91 % p -821.9	1.80764 99.73 % p -609.0	1.79568 99.71 % p -608.5	1.80764 99.73 % p -609.0	1.79568 99.71 % p -608.5
X-ray 2 mol	-7629498.5	-173.56	10.51	1.86100 99.91 % p -841.4	*1.85541 99.91 % p -828.6	1.82171 99.88 % p -675.1	1.80944 99.89 % p -674.3	1.80730 99.73 % p -612.5	1.79523 99.71 % p -612.1
	(-3814749.3 per one molecule)	4.11	177.93	1.84878 99.87 % p -781.0	1.86183 99.79 % p -821.0	1.81071 99.74 % p -553.5	1.79856 99.72 % p -553.0	1.80908 99.73 % p -615.8	*1.79731 99.71 % p -615.3

intramolecular interactions, which are the biggest for calculated molecules of the conformers **c** and **d**, block significantly the possibility of ether oxygens to participate in additional intermolecular interactions as co-ordination to metal ions. The stabilization energy values calculated about the orbital overlap of LP(O) of phosphoryl oxygen atoms and the two antibonding  $\sigma(\text{C-P})^*$  orbitals are lower (see Table 4) and the differences between orbital energies are bigger. The mainly p-character of these oxygen lone pair orbitals (Table 3) together with low participation in intramolecular hyperconjugation (Table 4) show behavior close to pure lone pair orbitals. Hence on the basis of the NBO analysis it could be concluded that phosphoryl oxygen atoms are more reactive and capable to coordinate than ether oxygens. Generally, the data presented in Table 4 shows that the two phosphoryl oxygen atoms belonging to one molecule of p-I have different reactivity. The close values for the stabilization energies and the differences of the orbital energies were only observed for the

molecules obtained from the optimization of the Z-matrix of X-ray data. On the basis of the data from the second-order perturbation theory analysis of the orbital donor-acceptor interactions it could be concluded that the more reactive to coordination is one of the two phosphoryl oxygen atoms per molecule and the most reactive molecule is that of the d-conformer, obtained after optimization in gas phase. The coordination through the ether oxygen atoms is less likely because of conjugation with the aromatic  $\pi$ -electrons.

In order to obtain additional chemical interpretation to the charge distribution in the optimized molecular structures and hence complete characterization of the electronic structure, the natural atomic charges and Mulliken charges were analyzed in the ground state. The data for the atomic charges obtained from the Mulliken population analysis [16] and molecular charge distribution in terms of NPA (Natural population analysis) charges (namely – nuclear charge minus summed natural populations

**Table 4.** Second-order perturbation theory analysis of the of the donor-acceptor interactions based on the NBO basis

Conformation number	Donor NBO (i)	Acceptor NBO (j)	E(2) <sup>a</sup> [KJ/mol]	E(j) – E(i) <sup>b</sup> [a. u.]	F(ij) <sup>c</sup> [a. u.]
a)	LP(O11)	BD*(C11-C12)	100.4	0.35	0.087
	LP(O11')	BD*(C11'-C13)	112.6	0.34	0.092
	LP1(O12)	BD*(P11-C15)	69.2	0.45	0.078
	LP2(O12)	BD*(P11-C14)	94.0	0.43	0.089
	LP1(O12')	BD*(P11'-C15')	68.2	0.45	0.078
	LP2(O12')	BD*(P11'-C14')	94.1	0.43	0.089
b)	LP(O11)	BD*(C11-C12)	101.0	0.35	0.087
	LP(O11')	BD*(C11'-C13)	112.7	0.34	0.092
	LP1(O12)	BD*(P11-C15)	67.6	0.45	0.078
	LP2(O12)	BD*(P11-C14)	94.1	0.43	0.089
	LP1(O12')	BD*(P11'-C15')	67.5	0.45	0.078
	LP2(O12')	BD*(P11'-C14')	92.8	0.44	0.089
c)	LP(O11)	BD*(C11-C12)	114.5	0.34	0.093
	LP(O11')	BD*(C11'-C13)	115.4	0.34	0.093
	LP1(O12)	BD*(P11-C15)	66.8	0.45	0.077
	LP2(O12)	BD*(P11-C14)	92.8	0.44	0.089
	LP1(O12')	BD*(P11'-C15')	68.5	0.45	0.078
	LP2(O12')	BD*(P11'-C14')	94.1	0.43	0.089
d)	LP(O11)	BD*(C11-C12)	114.5	0.34	0.093
	LP(O11')	BD*(C11'-C13)	114.5	0.34	0.093
	LP1(O12)	BD*(P11-C15)	66.8	0.45	0.077
	LP2(O12)	BD*(P11-C14)	92.9	0.44	0.089
	LP1(O12')	BD*(P11'-C15')	66.8	0.45	0.077
	LP2(O12')	BD*(P11'-C14')	92.9	0.44	0.089
e)	LP(O11)	BD*(C11-C12)	103.0	0.35	0.088
	LP(O11')	BD*(C11'-C13)	112.6	0.34	0.092
	LP1(O12)	BD*(P11-C15)	66.7	0.45	0.077
	LP2(O12)	BD*(P11-C14)	92.7	0.44	0.089
	LP1(O12')	BD*(P11'-C15')	66.7	0.45	0.077
	LP2(O12')	BD*(P11'-C14')	92.8	0.44	0.089
X-ray 1mol	LP(O11)	BD*(C11-C12)	114.1	0.34	0.092
	LP(O11')	BD*(C11'-C13)	103.8	0.34	0.088
	LP1(O12)	BD*(P11-C15)	80.7	0.45	0.085
	LP2(O12)	BD*(P11-C14)	91.3	0.43	0.088
	LP1(O12')	BD*(P11'-C15')	80.6	0.45	0.085
	LP2(O12')	BD*(P11'-C14')	91.25	0.43	0.088
X-ray 2 mol	LP(O11)	BD*(C11-C12)	100.8	0.35	0.087
	LP(O11')	BD*(C11'-C13)	115.5	0.34	0.093
	LP1(O12)	BD*(P11-C15)	72.0	0.46	0.081
	LP2(O12)	BD*(P11-C14)	83.0	0.45	0.085
	LP1(O12')	BD*(P11'-C15')	80.1	0.45	0.085
	LP2(O12')	BD*(P11'-C14')	92.2	0.43	0.088
	LP(O21)	BD*(C21-C22)	113.3	0.33	0.091
	LP(O21')	BD*(C21'-C23)	107.9	0.34	0.091
	LP1(O22)	BD*(P21-C25)	78.9	0.45	0.084
	LP2(O22)	BD*(P21-C24)	91.7	0.43	0.088
	LP1(O22')	BD*(P21'-C25')	81.4	0.45	0.085
	LP2(O22')	BD*(P21'-C24')	89.0	0.43	0.087

a) E(2) means energy of hyperconjugative interactions;

b) E(j) – E(i) – Energy difference between donor and acceptor i and j NBO orbitals.

c) F(i, j) is the Fock matrix element between i and j NBO orbitals.

of NAOs on the atom) [14d] are presented on Figures 3 and 6. The Mulliken's procedure, the most widely used method for representation of the electron density distribution was performed at each level of theory using variety of basis sets. The analysis of molecular charge distribution supported the description of electron-pair "bonding" unit was done at DFT level of theory using 6-31G(d) basis set. The calculations obtained for the molecule of *p*-I in gas phase and using Z-matrix of the solid state at different level of theory proved the gain of more negative charges from the phosphoryl oxygens and hence higher reactivity. The comparison of the charge distribution in the conformers (Fig. 6) shows that they differ only in respect to the charges on the oxygen and phosphorus atoms.

These differences could be explained with different degree of conjugation in the chain P-CH<sub>2</sub>-O-Ar-O-CH<sub>2</sub>-P as a consequence of different spatial location of the substituents in the five conformers. On the basis of the charge distribution, it is worth comparing the reactivity of the phosphoryl O-atoms obtained for the optimized structures in gas phase and solid state using DFT calculations. The most reactive is one of the phosphoryl O-atoms belonging to one of the two molecules obtained after optimization of the X-ray data for the two molecules in the unit cell. It should be emphasized that the electron density distribution on the two molecules obtained after X-ray data optimization differs significantly and the distribution on the molecule A is close to the data obtained from optimization in gas phase.

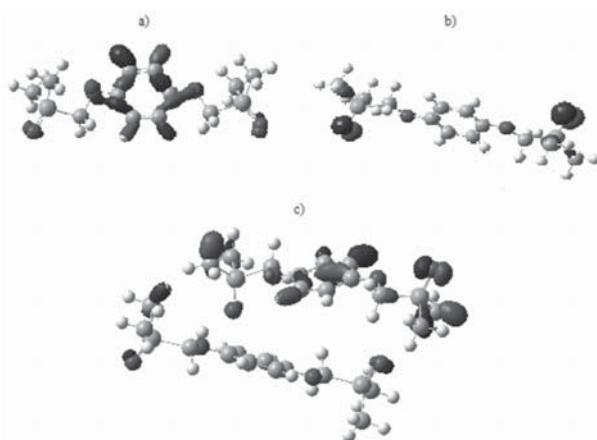


**Fig. 7.** Frontier molecular orbitals, studied by RHF/6-311G(d) level of theory as the optimization was done in: a) gas phase; b) using the Z-matrix of X-ray data for an isolated A molecule at B3LYP/6-31G(d); c) using the Z-matrix of X-ray data of the two molecules in the unit cell at B3LYP/6-31G(d)

This trend was proved again using RHF/6-311G(d) level of theory, as can be seen from the computed electronic density map presented on Fig. 7.

To clarify the differences in the spatial location of the substituents in the molecule of *p*-I obtained after optimization in gas phase and that from X-ray single crystal refinement, and their influence on the reactivity, the IR spectrum of the polycrystalline sample of the studied compound was re-

**Table 5.** Selected experimental and calculated frequencies (B3LYP/6-311G(d) of 1,4-bis(dimethylphosphinylmethyleneoxy)benzene

Experimental	Calculated			Assignment
	gas phase	X-ray of 1 molecules	X-ray of 2 molecules	
–	1597	–	–	v(Ar(C=C))
	1566	–	1501	
1501	1485	1499	1499	
1437	–	–	1412	
1416	1403	1411	1411	
1221	1212	1216	1219	v(C <sub>Ar</sub> -O)
	1196	1204	1217	
			1205	
			1203	
1163	1165	–	1177	v(P=O)
	1163	1175	1175	
			1173	
1043	1027	1047	1047	v(CH <sub>2</sub> -O)
932	1015	932	1044	
896		924		
866	933	875	935	δ(CH <sub>3</sub> -P-CH <sub>3</sub> ) + δ(CH <sub>2</sub> -P-CH <sub>3</sub> )
835	929	846	876	
	905		868	
	849		847	

corded. The observed experimental IR frequencies were compared with theoretically predicted vibrational spectra (Table 5). The calculated vibrational frequencies proved the correctness of the structural optimizations. The assignments of the bands of the experimental IR spectrum are made in accordance with IR data and NCA published for tertiary phosphine oxides (Table 5) [5b,16]. The comparison of the experimental with the calculated data shows coincidence in different regions. The observed P=O stretching band coincides with calculated frequencies for optimized molecule in gas phase as well as the calculated spectrum using X-ray data is close to experimental spectrum in the range  $\nu$  H<sub>2</sub>C-O and  $\delta$ ((CH<sub>3</sub>-P-CH<sub>3</sub>)) bands. Therefore, it could be assumed that more than one conformer present in real polycrystalline sample.

## CONCLUSION

The crystal structure of 1,4-bis(dimethylphosphinylmethylenoxy)benzene reveals the existence of two symmetrically non equivalent molecules (A and B) in the asymmetric unit. To estimate fully its electronic structure and coordination behavior, theoretical analysis was applied. All theoretical found bond lengths and bond angles are in good agreement with X-ray refinements values and large differences were observed for the dihedral angles related to the location of the two substituents in respect to the plane of the benzene ring. To explain the structural mobility due to the three single bonds C(Ar)-O-C-P in each substituent, the conformational analysis was applied. Five relevant lowest energy conformers were found as the estimated conformational energy differences are very small. The coordination ability of the compound was evaluated in terms of Natural Bond Orbitals, Mulliken charges and analysis of the frontier molecular orbitals. The highest reactivity was proved for the phosphoryl O-atoms. The calculated vibrational frequencies of the compound were used to check the structural optimizations and to compare with experimental data. The most stable conformer was obtained by computation in gas phase, because free from the intermolecular forces, the molecule relaxes to the nearest local minima in the potential surface. The steric hindrance of the bulky methyl groups is an acting force for the arrangement in the crystal structure. In the polycrystalline sample, conformers with different location of the substitutes are possible.

## Supplementary Materials

CCDC 805281 contains the supplementary crystallographic data for this paper. This data can be obtained

free of charge via [www.ccdc.cam.ac.uk/data\\_request/cif](http://www.ccdc.cam.ac.uk/data_request/cif), by e-mailing [data\\_request@ccdc.cam.ac.uk](mailto:data_request@ccdc.cam.ac.uk), or by contacting The Cambridge Crystallographic Data Centre, 12 Union Road, Cambridge CB2 1EZ, UK; fax: +44(0)1223-336033.

**Acknowledgements:** The financial support by the Bulgarian National Science Fund (Ministry of Education, Youth and Science, Bulgaria) under contract No DRNF 02/1 is gratefully acknowledged.

## REFERENCES

1. S. Varbanov, T. Tosheva, G. Borisov, *Phosphorus, Sulfur & Silicon*, **63**, 397 (1991).
2. a) R. Nassar, B. C. Noll, K. W. Henderson, *Polyhedron*, **23**, 2499 (2004); b) N. M. A. El-Rahman, L. S. Boulos, *Molecules*, **7**, 81 (2002).
3. a) B. A. Trofimov, S. F. Malysheva, N. K. Gusarova, V. A. Kuimov, N. A. Belogorlova, B. G. Sukhov, *Tetrahedron Letters*, **49**, 3480 (2008); b) A. R. Daniewski, L. M. Garofalo, S. D. Hutchings, M. M. Kabat, W. Liu, M. Okabe, R. Radinov, G. P. Yiannikouros, *J. Org. Chem.*, **67**, 1580 (2002).
4. R. Lerebours, Ch. Wolf, *Org. Lett.*, **9**, 2737 (2007); b) A. C. Durrell, H. B. Gray, N. Hazari, Ch. D. Incarvito, J. Liu, E. C. Y. Yan, *Cryst. Growth & Des. Communication*, **10**, 1482 (2010).
5. a) G. Borisov, G. Varbanov, L. M. Venanzi, A. Albinati, F. Demartin, *Inorganic Chemistry* **33**, 5430 (1994); b) N. Trendafilova, I. Georgieva, *Vibrational Spectroscopy*, **20**, 133 (1999); c) V. Vassileva, G. Gencheva, E. Russeva, S. Varbanov, R. Scopelliti, E. Tashev, *Inorg. Chim. Acta*, **358**, 2671 (2005); d) L. Le Saulnier, S. Varbanov, R. Scopelliti, M. Elhabiri, J.-Cl. G. Bünzli, *J. Chem. Soc., Dalton Trans.*, 3919 (1999); e) L. N. Puntus, An.-S. Chauvin, S. Varbanov, J.-Cl. G. Bünzli, *Eur. J. Inorg. Chem.*, 2315 (2007).
6. a) F. de M. Ramirez, S. Varbanov, C. Cécile, G. Muller, N. Fatim-Rouge, R. J.-Cl. G. Bünzli, *J. Phys. Chem. B*, **112**, 10976 (2008); c) J. D. Law, K. N. Brewer, R. S. Herbst, T. A. Todd, D. J. Wood, *Waste Management*, **19**, 27 (1999); d) Z. Chan, Y. Yan-Zhao, Z. Tao, H. Jian, L. Chang-Hong, *J. Radioanal. Nucl. Chem.*, **265**, 419 (2005).
7. a) R. Petrova, B. Shivachev, D. Tsekova, P. Gorolomova, V. Ilieva, S. Varbanov, G. Gencheva, *1<sup>st</sup> National Crystallographic Symposium, Sofia*, p. 129 (2009); b) G. Gencheva, D. Tsekova, P. Gorolomova, V. Ilieva, R. Petrova, B. Shivachev, T. Tosheva, E. Tashev and S. Varbanov, *Second Workshop on Size-Dependent Effects in Materials for Environmental Protection and Energy Application*, p. 51 (2010); c) V. Ilieva, R. Petrova, B. Shivachev, P. Gorolomova, D. Tsekova, T. Tosheva, E. Tashev, S. Varbanov, G. Gencheva, *11<sup>th</sup> National Crystallographic Symposium, Sofia*, p. 49 (2010).
8. a) Enraf-Nonius, CAD-4 EXPRESS Software. Enraf-Nonius, Delft, The Netherlands (1994); b) K. Harms and S. Wocadlo, XCAD4. Program for Processing

- CAD-4 Diffractometer Data. University of Marburg, Germany (1995); c) G. M. Sheldrick, *Acta Cryst.*, **A64**, 112 (2008).
9. a) A. D. Becke, *J. Chem. Phys.*, **97**, 2155 (1992); b) A. D. Becke, *J. Chem. Phys.*, **98**, 9173 (1992); c) C. T. Lee, W. T. Yang, R. G. Parr, *Phys. Rev.*, **B**, **37**, 785 (1988).
10. a) C. C. Roothan, *Rav. Mod. Phys.*, **23**, 69 (1951); b) G. G. Hall, *Proc. Roy. Soc.*, **205**, 541 (1951).
11. C. Møller, M. S. Plesset, *Phys. Rev.*, **46**, 618 (1934).
12. M. J. Frisch; G. W. Trucks; H. B. Schlegel; G. E. Scuseria; M. A. Robb; J. R. Cheeseman; Jr. J. A. Montgomery; T. Vreven; K. N. Kudin; J. C. Burant; J. M. Millam; S. S. Iyengar; J. Tomasi; V. Barone; B. Mennucci; M. Cossi; G. Scalmani; N. Rega; G. A. Petersson; H. Nakatsuji; M. Hada; M. Ehara; K. Toyota; R. Fukuda; J. Hasegawa; M. Ishida; T. Nakajima; Y. Honda; O. Kitao; H. Nakai; M. Klene; X. Li; J. E. Knox; H. P. Hratchian; J. B. Cross; V. Bakken; C. Adamo; J. Jaramillo; R. Gomperts; R. E. Stratmann; O. Yazyev; A. J. Austin; R. Cammi; C. Pomelli; J. W. Ochterski; P. Y. Ayala; K. Morokuma; G. A. Voth; P. Salvador; J. J. Dannenberg; V. G. Zakrzewski; S. Dapprich; A. D. Daniels; M. C. Strain; O. Farkas; D. K. Malick; A. D. Rabuck; K. Raghavachari; J. B. Foresman; J. V. Ortiz; Q. Cui; A. G. Baboul; S. Clifford; J. Cioslowski; B. B. Stefanov; G. Liu; A. Liashenko; P. Piskorz; I. Komaromi; R. L. Martin; D. J. Fox; T. Keith; M. A. Al-Laham; C. Y. Peng; A. Nanayakkara; M. Challacombe; P. M. W. Gill; B. Johnson; W. Chen; M. W. Wong; C. Gonzalez; and J. A. Pople; Gaussian, Inc., Wallingford CT, Gaussian 09 (Revision-A.01); Gaussian, Inc.: Pittsburgh, PA, 2009.
13. S. F. Boys, F. Bernardi, *Molecular Physics*, **19**, 553 (1970).
14. a) J. P. Foster, F. Weinhold, *J. Am. Chem. Soc.*, **102**, 7211 (1980); b) A. E. Reed, F. Weinhold, *J. Chem. Phys.*, **78**, 4066, (1983); c) A. E. Reed, R. B. Weinstock, F. Weinhold, *J. Chem. Phys.*, **83**, 735, (1985); d) A. E. Reed, F. Weinhold, *J. Chem. Phys.*, **83**, 1736, (1985); e) A. E. Reed, L. A. Curtiss, F. Weinhold, *Chem. Rev.*, **88**, 899, (1988).
15. a) A. C. Durrell, H. B. Gray, N. Hazari, Ch. D. Incarvito, J. Liu, E. C. Y. Yan, *Cryst. Growth & Design*, **10**, 1482 (2010); b) H. K. Wang, *Acta Chem. Scand.*, **19**, 879 (1965); c) V. Chandrasekhar, R. Azhakar, *Cryst. Eng. Comm.*, **7**, 346 (2005).
16. R. S. Mulliken, *J. Chem. Phys.* **23** (1955) 1833.
17. K. Nakamoto, *Infrared and Raman Spectra of Inorganic and Coordination Compounds-Part B*, 5<sup>th</sup> ed., John Wiley&Sons, New York, NY, USA (1997).

## ТЕОРЕТИЧНО И ЕКСПЕРИМЕНТАЛНО ИЗСЛЕДВАНЕ ВЪРХУ КООРДИНАЦИОННАТА СПОСОБНОСТ НА 1,4-БИС(МЕТИЛФОСФИНИЛМЕТИЛЕНОКСИ)БЕНЗЕН

П. Й. Гороломова<sup>1</sup>, Р. П. Николова<sup>2</sup>, Б. Л. Шивачев<sup>2</sup>, В. И. Илиева<sup>1</sup>, Д. Ц. Цекова<sup>1</sup>,  
Т. Д. Тошева<sup>3</sup>, Е. С. Ташев<sup>3</sup>, С. Г. Варбанов<sup>4</sup>, Г. Г. Генчева<sup>1</sup>

<sup>1</sup> Химически факултет, Софийски университет

<sup>2</sup> Институт по минералогия и кристалография, Българска академия на науките

<sup>3</sup> Институт по полимери, Българска академия на науките

<sup>4</sup> Институт по органична химия с Център по фитохимия, Българска академия на науките

Постъпила на 28 януари, 2011 г.; приета на 22 април, 2011 г.

(Резюме)

Молекулната, кристалната структура и координационната способност на 1,4-бис(метилфосфинилметиленокси)бензен са изучени експериментално, с методите на рентгеновата дифракция и ИЧ- спектроскопия, и теоретично - с *ab initio* RHF/6-311G(d), MP2/6-311G(d) методите, както и с DFT B3LYP/6-311G(2df,2p). Съединението кристализира в триклинна кристална система, с пространствена група на симетрия P-1. Квантово-химичните пресмятания за газова фаза показаха, че съединението може да съществува в няколко слабо различаващи се по енергия стабилни конформери, описани чрез диедричния ъгъл C<sub>Ar</sub>-C<sub>Ar</sub>-O-C. Координационните свойства бяха характеризирани с помощта на NBO-анализ, оценка на Мъликеновите заряди и разпределението на електронната плътност върху естествените несвързващи LP молекулни орбитали. Получените резултати показаха, че с най-висока координационна способност се отличават фосфорилните O-атоми. Най-стабилният конформер беше получен за газова фаза. Данните от рентгеновата дифракция показаха, че подреждането на молекулите в кристалната опаковка се определя от стеричното отблъскване между обемистите метилови групи от заместителите.